Accepted Manuscript

Electrochemical synthesis and characterization of poly(*o*-toluidine) as high energy storage material

Milica M. Gvozdenović, Braninir Z. Jugović, Bojan M. Jokić, Enis S. Džunuzović, Braninimir N. Grgur

PII:	S0013-4686(19)31191-0
DOI:	10.1016/j.electacta.2019.06.046
Reference:	EA 34353
To appear in:	*Electrochimica Acta*
Received Date:	25 March 2019
Accepted Date:	09 June 2019

Please cite this article as: Milica M. Gvozdenović, Braninir Z. Jugović, Bojan M. Jokić, Enis S. Džunuzović, Braninimir N. Grgur, Electrochemical synthesis and characterization of poly(*o*-toluidine) as high energy storage material, *Electrochimica Acta* (2019), doi: 10.1016/j.electacta.2019.06.046

Electrochemical synthesis and characterization of poly(*o*-toluidine) as high energy storage material

Milica M. Gvozdenović[1,*], Braninir Z. Jugović[2], Bojan M. Jokić[1, 3], Enis S. Džunuzović[1], Braninimir N. Grgur[1]

[1]Faculty of Technology and Metallurgy, University of Belgrade, Karnegijeva 4, 11120 Belgrade, Serbia

[2]Insitute of Technical Science, Serbian Academy of Science and Arts, Knez Mihajlova 35, 11000 Belgrade, Serbia

[3]Faculty of Applied Arts, University of Arts in Belgrade, Kralja Petra 4, 11000 Belgrade, Serbia

*corresponding author: popovic@tmf.bg.ac.rs (M. Gvozdenović)

Abstract

Poly(*o*-toluidine) (POT) is electrochemically synthesized on graphite electrode at constant current density of 1.5 mA cm^{-2} from aqueous electrolyte of 1.0 mol dm^{-3} H_2SO_4 and 0.25 mol dm^{-3} *o*-toluidine. Electrochemical characterization of POT electrode is performed using cyclic voltammetry, Mot Schottky analysis and galvanostatic measurements at different currents. POT electrode exhibited high energy storage features, with specific energy up to 17.5 Wh kg^{-1} and specific power up to 3300 W kg^{-1}. Cyclic stability exceeding 90% is obtained over 2000 charge/discharge cycles at 13.1 A g^{-1} indicating the perspective application of POT electrode as energy storage material.

Keywords: electrochemical polymerization, poly(*o*-toluidine), specific energy, specific power

1. Introduction

Energy originated from both renewable and alternative sources can be efficiently stored electrochemically. Classical electrochemical storage systems include electrochemical double layer capacitors (EDLC) and batteries. EDLC are characterized by high specific power up to 90 kW kg^{-1} [1], but suffers from low specific energy outputs in the range of a few Wh kg^{-1}. On contrary, batteries deliver high specific energy, but significantly slower comparing to EDLC, leading to low specific power typically in the range of 0.2~1.8 kW kg^{-1} [1]. A promising alternative to EDLC is based on usage of pseudocapacitive materials, such as RuO_2, MnO_2 [2] and other electrochemically active materials with good charge storage ability, whose electrochemical behavior is often in literature incorrectly denoted as been pseudocapacitive, like found with some metal oxides and intrinsically conductive polymers (ICP's) [2–6]. As nicely explained by Brousee et al. [2] the term "pseudocapacitive" can be exclusively attributed to material with Faradic nature of the charge storage process and rectangular shaped cyclic voltammograms as observed with classical carbon capacitive electrodes. Owing to low cost, environmental stability, high electrical conductivity of the doped state and ease of the both chemical and electrochemical synthesis ICP's are considered as a promising energy storage materials [5–9]. Bearing in mind that the charge storage mechanism of ICP's originates from redox behavior and linearly shaped charge/discharge curves, the term "psudocapacitve" is incorrectly [2], but extensively used in the literature, although these materials exhibit typical peak-shaped cyclic voltammograms. The high charge storage ability of ICP's is based on fast and reversible doping/dedoping reactions of the ions in the polymer backbone. Among numerous ICP's polyaniline (PANI) is probably the most widely investigated [7]. Electrochemical performance of PANI based electrodes is strongly dependent on various parameters such as: preparation conditions, electrolyte, potential

window, discharge rate regime etc. Although literature data suggests that it is possible to achieve satisfactory values of the specific capacity and both specific energy and power, the major obstacle for practical application of PANI is poor cycling stability leading to a low capacity retention as a consequence of significant volume alternation due to swelling and shrinking of the polymer by doping (oxidation) and dedoping (reduction) of ions of the polymer backbone [6]. Another well-known disadvantage of the practical application of PANI is related to the appearance of degradation products at potentials around 0.5 V [10]

Numerous approaches are applied in order to improve performance of PANI, most of them are related to formation of PANI composites by deposition on high surface area carbon materials [5–7,11–14].

It is reported in the literature that ICP's derived from substituted anilines had exhibit improvement of characteristics comparing to parent polymer. For example it is shown that poly(o-toluidine) (POT) obtained by oxidative polymerization of methyl substituted aniline, had good conductivity, electrochromic characteristics thermal and environmental stability [15], efficient electrocatalytic properties for oxygen reduction [16], and seemed attractive for application in Schottky diodes [17], organic solar cells [18], as well as in the corrosion protection [19–21]. According to studies by Bilal et al. [22,23] devoted to investigations of electrochemical and spectroelectrochemical properties of POT, it is shown that POT also existed in different oxidation forms dependent on electrode potential with insulator to conductor transitions from leucoemeraldine like state to emeraldine salt and conductor to insulator transition from emeraldine salt to perningraniline state during electrochemical doping induced by increase of the potential.

Having in mind similar redox behavior of POT and fact that, according to our knowledge, charge storage behavior of POT is not investigated before, the aim of this work is to investigate electrochemical synthesis and possible to investigate energy storage

characteristics of POT with special emphasis to it cyclic characteristics in forced current and potential regime.

2. Experimental

Electrochemical formation of poly(*o*-toluidine) (POT) electrode is achieved by the oxidative polymerization of *o*-toluidine (p.a. Aldrich) monomer on cylindrically shaped graphite electrode (S = 0.2 cm^2) from aqueous electrolyte containing 0.25 mol dm^{-3} *o*-toluidine (p.a. Merck) and 1.0 mol dm^{-3} H_2SO_4 (p.a. Merck) at constant current density of 1.5 mA cm^{-2} with polymerization charge of 1 mAh cm^{-2} (2400 s). Prior to the electrochemical polymerization, *o*-toluidine is distilled under reduced pressure, while graphite electrode is mechanically polished with different graded emery papers and polishing alumina on polishing cloths.

Electrochemical characterization of POT electrode is performed in 1.0 mol dm^{-3} H_2SO_4 by cyclic voltammetry technique, Mott Schottky analysis at a frequency of 1 Hz and galvanostatic charge/discharge experiments at different currents. In order to achieve complete dedoping, prior to the cyclic voltammetry and Mott Schottky experiments, the electrode is held at the cathodic potential of –0.6 V during 180 s in order to be completely dedoped. Electrochemical experiments are performed at ambient temperature (22 ± 1 °C) in a standard three-compartment electrochemical cell with Pt mesh as a counter and saturated calomel (SCE) as a reference electrode. The experiments are conducted using Gamry Potentiostat/Galvanostat ZRA 1010E equipped by suitable Electroanalyst software and connected to a PC.

UV-Vis spectroscopy measurements of electrochemically formed POT are recorded using LLG Uni SPEC 2 at 0.2 nm resolution. Prior to the spectroscopy measurements POT is dissolved in N-methil-2-pirrolidon (HPLC grade, Merck).

Scanning electronic micrograph images of electrochemically formed POT are recorded by field emission scanning electron microscope SEM MIRA 3 TESCAN at 10 kV.

3. Results and discussion

Electrochemical synthesis of poly(*o*-toluidine) (POT) on graphite electrode from an aqueous electrolyte containing 0.25 mol dm^{-3} *o*-toluidine and 1.0 mol dm^{-3} H_2SO_4 at a constant current density of 1.5 mA cm^{-2} with polymerization charge of 1 mAh cm^{-2} (2400 s) is shown in Fig. 1.

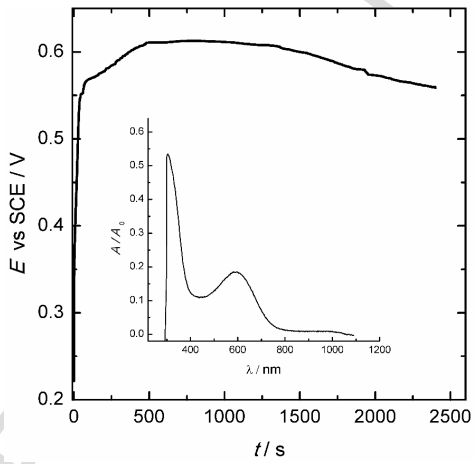

Fig.1. Galvanostatic (1.5 mA cm^{-2}) electrochemical polymerization of *o*-toluidine in 0.25 mol dm^{-3} *o*-toluidine and 1.0 mol dm^{-3} H_2SO_4. Inset: UV-vis absorption spectra of POT.

Electrochemical polymerization of *o*-toluidine (OT) in sulfuric acid occurring together with insertion (doping) of sulfate ions according to:

$$n\mathrm{OT} + n(y/2)\mathrm{SO_4^{2-}} \rightarrow [\mathrm{POT}^{y+}(\mathrm{SO_4^{2-}})_{y/2}]_n + 2n\mathrm{H^+} + (2+y)n\mathrm{e} \quad (1)$$

with *y* referring to doping degree defined as the ratio of the charges in the polymer chain and the number of the monomer unit.

Electrochemical polymerization of OT proceeds with a fast increase of the potential to about 0.55 V, followed by a further slow increase of the potential to 0.60 V after which nearly constant values of the potential are observed. The values of the potentials necessary to growth the polymer film on the electrode are slightly lower comparing to polyaniline [24] probably due to the presence of ortho positioned methyl group which is moderate activator of electrophilic aromatic substitution, through its inductive effect, leading to the faster electrochemical reaction.

It is reasonable to assume that electrochemical polymerization of OT follows generally excepted mechanism of the oxidative radical polymerization [25]. Accordingly, the first step would involve the formation of OT cation radicals through monomer oxidation at the anode as schematically presented in Fig. 2.

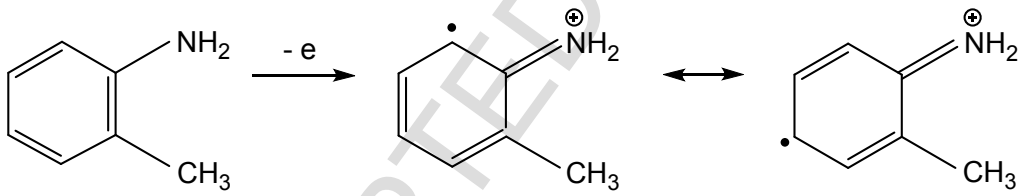

Fig. 2. Formation of OT cation radicals at the anode.

In further steps, the coupling of radicals with loss of protons and recovery of the aromatic structure through the formation of dimmers, and lately oligomers occurs. Chain propagation is achieved by coupling of oligomers and OT cation radicals. The presence of two activating groups on benzene: amino (strongly activating by resonance effect) and methyl (moderately activating by inductive effect), activates electrophilic attack at ortho and para positions with

the coupling of the radicals predominately at p-p positions. The ortho positioned methyl group however introduces some steric hindrances manifested as a slight increase of the polymerization potential observed at the galvanostatic curve, instead of plateau potential observed with polyaniline galvanostatic synthesis [8].

A UV-vis absorbance spectrum of POT is given in inset of Fig 1. The spectrum is taken upon dissolution in N-methyl-2-pyrrolidone and therefore refers to the polymer in dedoped form. As it can be seen, the spectrum of POT is characterized by the existence of the first maximum at 590 nm, often reported as Q peak referring to electron excitation from the highest occupied molecular orbital, HOMO, of the benzenoid rings to the lowest unoccupied molecular orbital, LUMO, of the quinonoide rings. The second maximum at 309 nm, known as B peak, is assigned to $\pi \rightarrow \pi^*$ transition of the benzene ring electrons. Q peak characteristic to emeraldine state, located at 630 nm [26] in polyaniline spectra, is shifted to a lower wavelength at around 590 nm in POT spectra, while B peak located at 320 in polyaniline [26] is moved to 306 nm in POT spectra. According to work of Yang et al., the ratio of B and Q peaks (B/Q) enables determination of the oxidation levels [27]. Following the proposed procedure, the estimated oxidation level of POT is around 0.47 which is close to the theoretical value of the emeraldine like state.

Scanning electron micrographs of electrochemically synthesized POT at different magnifications are given in Fig. 3.

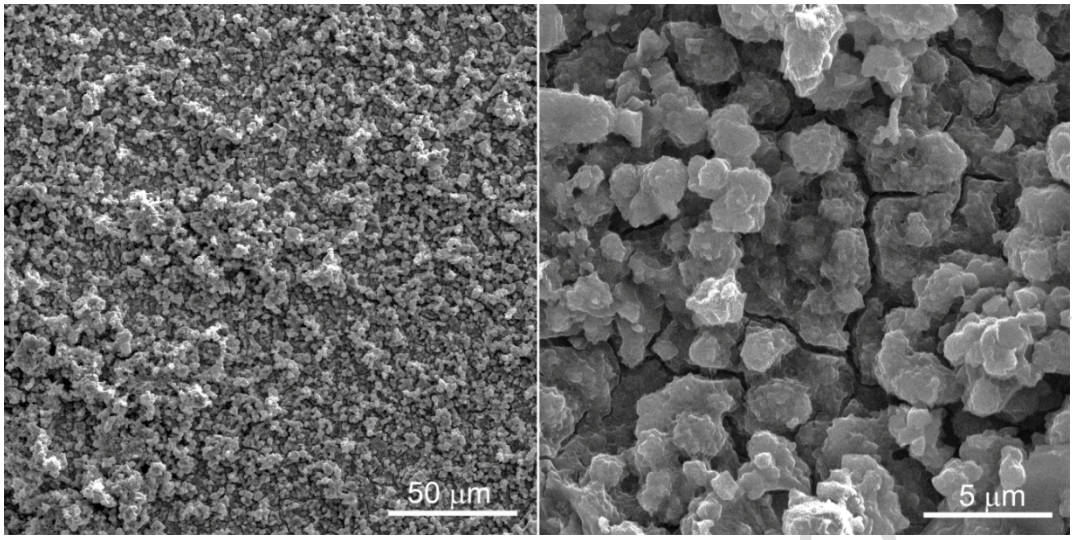

Fig. 3. SEM micrographs of electrochemically synthesized POT at different magnifications.

It can be seen from Fig. 3, that electrochemically formed POT is uniformly deposited on the graphite electrode. It is observed that particles of POT have spheroidal, flaky like morphology which is different from usual nanosized fibrous network characteristic to polyaniline [28-30]. The reason for the formation of particles of nonfibrous morphology can be explained by more common heterogeneous nucleation and the propensity of the polyaniline derivatives to form spherical particles due to both steric and electronic effects of the substituent such as presence of the methyl group [31,32].

In order to investigate the influence of the potential on existence and conductivity of different oxidation forms of POT, cyclic voltammogram together with capacitance and impedance at 1 Hz derived from the Mott Schottky experiments of POT film is recorded in the potential range of –0.5 V to 0.5 V and given in Fig. 4.

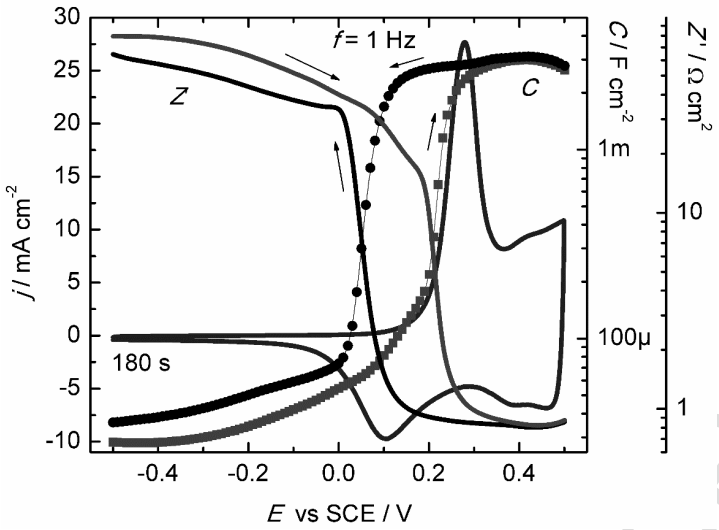

Fig. 4. Cyclic voltammogram and capacitance and impedance at 1 Hz of POT electrode in 1.0 mol dm^{-3} H_2SO_4 in the potential range between –0.5 and 0.5 V.

From the cyclic voltammogram, shown in Fig 4, it can be clearly seen that transition of leucoemeraldine like state to conductive emeraldine salt is observed with POT, with anodic potential characteristic to emeraldine salt at around 0.27 V. Doping of leucomeraldine like state is followed by increase of the conductivity of POT film which resulted in decrease of the impedance and increase of the film capacitance, as seen in Fig 4. On contrary, as seen in cathodic part in Fig. 4, dedoping of emeraldine state to leucoemeraldine, induced increase of the impedance and decrease of the capacitance caused by loss of the film conductivity owing to dedoping reaction. The similar results at 1 Hz were obtained for polyaniline, indicating the same charge storage mechanism [33].

According to the recent studies reported by Contractor and Juvekar, the band structure of polyaniline is also dependent on potential, with most of the available capacitance over 70 % referring to polaron and polaron lattice states occurring in the potential region between 0.15 and 0.50 V [34]. This potential region is related to the existence of half oxidized form of the emeraldine salt.

Because the structural behavior of polyaniline is mainly treated for doping by monovalent anions, for the analysis of both polymerization charge and available charge for doping by divalent sulphate anions it is necessary to consider that two POT polymer units, both consisted of four monomer units, will share two sulphate anions between parallel chains, as given schematically in Fig 5.

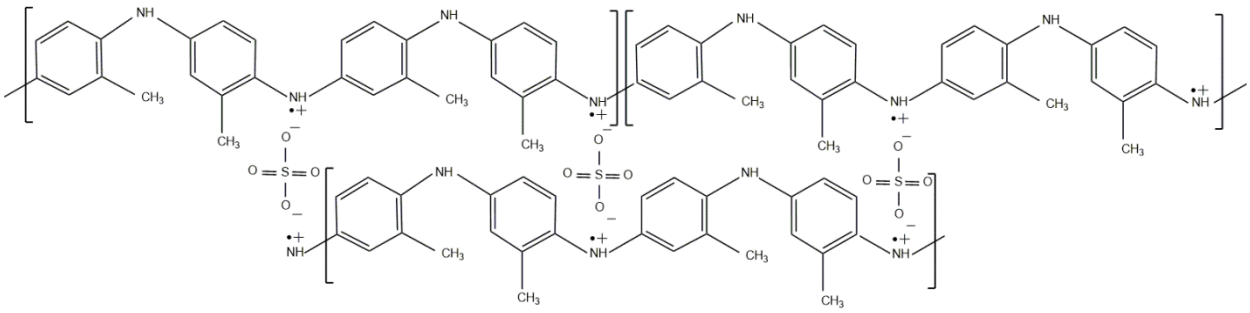

Fig. 5. Emeraldine salt like state of POT with shared sulphate anions.

However, the polymer unit is still doped by two anions, so that the polaronic structure related to half-oxidized emeraldine state (y = 0.5) is preserved. Because these anions are shared by two polymer units, the whole polymer is doped by half of the divalent anions, namely $n{\cdot}y/2$ anions to maintain charge neutrality [8].

The polymerization charge, Q_p, of the electrochemical formation of POT, assuming that the current efficiency of the polymerization process is close to 100%, Q_p can be expressed by:

$$Q_p = I_p t_p = (2 + y)neF \tag{2}$$

where y refers to doping degree, while I_p and t_p are polymerization current and time respectively.

Having in mind that dedoping/doping, i.e. reduction/oxidation reaction, of POT by sulphate anions is given as:

$$[\mathrm{POT}^{y+}(\mathrm{SO_4}^{2-})_{y/2}]_n + (y/2)ne \underset{\text{doping}}{\overset{\text{dedoping}}{\Leftrightarrow}} [\mathrm{POT}^{0}]_n + n(y/2)\mathrm{SO_4}^{2-} \tag{3}$$

while the theoretically available charge capacity can be given as:

$$Q = It = (y/2)neF \tag{4}$$

These two charges are correlated as:

$$Q = \frac{(y/2)}{2+y} Q_{\mathrm{p}} = \frac{(y/2)}{2+y} I_{\mathrm{p}} t_{\mathrm{p}} \tag{5}$$

Hence, for the given conditions, the theoretical dedoping charge corresponds to ~0.1 mAh cm^{-2} The mass of POT obtained by polymerization charge of $I_{\mathrm{p}}t_{\mathrm{p}}$, can be estimated relaying on Faraday law, using:

$$m_{\mathrm{POT}} = \frac{I_{\mathrm{p}} t_{\mathrm{p}} [M_{\mathrm{OT}} - 2M_{\mathrm{H^+}} + (y/2) M_{\mathrm{SO_4^{2-}}}]}{(2+y)F} \tag{6}$$

where M stands for molar masses of OT monomer, sulphate anion, and proton. The mass of POT for the given polymerization charge of 1 mAh cm^{-2}, and assuming emeraldine salt state, is estimated to 1.9 mg cm^{-2}.

Charge/discharge curves of POT electrode obtained with different current densities, with charge potential limit of 0.5 V and discharge potential limit of – 0.3 V are given in Fig. 6a., while charge/discharge over recalculated areal capacity are given in Fig 6b. The shape of the charge/discharge curves is rectangular, in the potential range 0.2 to 0.5 V for charge and 0.5 V to ~0 V for discharge. Fast decreases of the potential during discharge below ~0 V is connected with solid state diffusion limitations of counter ions.

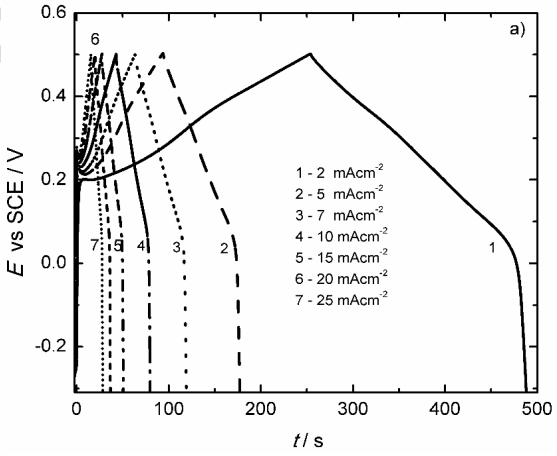

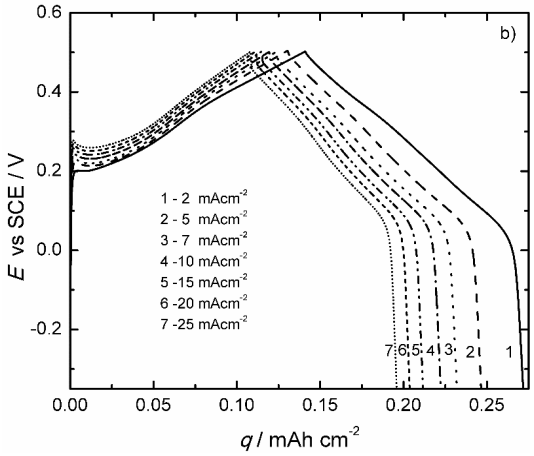

Fig. 6. Charge/discharge curves of POT electrode in 1.0 mol dm^{-3} H_2SO_4 with different current densities as marked in figure, a) over time and b) over recalculated capacity.

Charge/discharge capacities are dependent on applied specific currents, as it can be seen from Fig. 7. Maximally obtained specific values of 75 mAh g^{-1} for charge and 65 mAh g^{-1} for discharge are obtained with a lowest specific current of 1 A g^{-1}, while 56 mAh g^{-1} (charge) and 44 mAh g^{-1} (discharge) are obtained with a highest specific current of 13.1 A g^{-1}. However, the Coulombic efficiency in the range 90% to 80% is slightly affected by charge/discharge current, as seen in inset of Fig. 7.

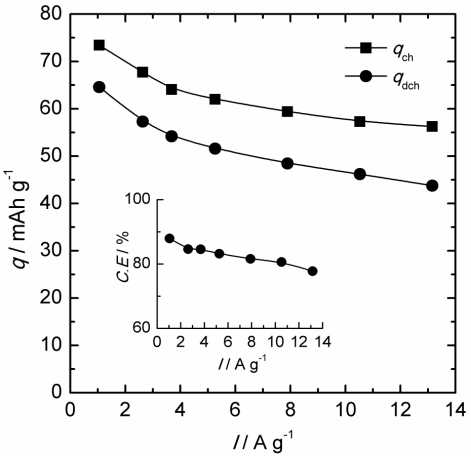

Fig. 7. The dependences of charge, q_{ch}, and discharge, q_{dch}, capacities on specific current. Insert: The dependence of Coulombic efficiency on specific current.

For the practical application of the electrode material parameters such as: specific energy and specific power, should be also considered.

Figure 8 shows dependence of specific energy over specific power, often reported as Ragone plot.

Specific energy, w (Wh kg^{-1}) and specific power P (W kg^{-1}) are determined by the integration of the potential over time dependences from Fig. 6a at constant specific discharge current, I (A g^{-1}), using their integral forms:

$$w = \frac{I}{3600}\int_0^t E\mathrm{d}t \tag{7}$$

$$P = \frac{I}{t}\int_0^t E\mathrm{d}t \tag{8}$$

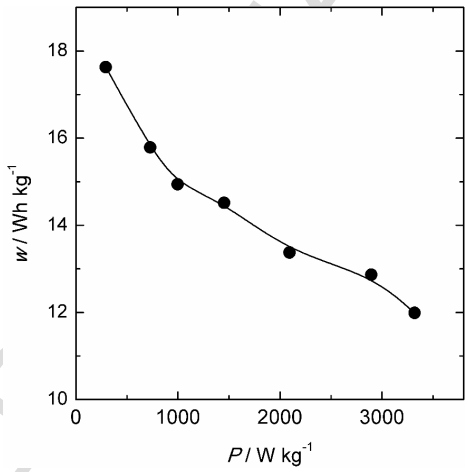

Fig.8. Ragone plot of POT electrode.

As seen from Fig. 8, specific energy decreased from 17.5 Wh kg^{-1} to 12 Wh kg^{-1}, while specific power increased from 300 W kg^{-1} to 3300 W kg^{-1}, with an increase of the discharge specific current. The value of the specific energy of 17.5 Wh kg^{-1} at 1 A g^{-1} are larger than those obtained for newly reported chemically synthesized nanostructured polyaniline (12.5 Wh kg^{-1} at 1 A g^{-1}) [35] or polyaniline composites (10.9 Wh kg^{-1} at 1 A g^{-1})

[36]. The values of specific power of 300 W kg^{-1} at 1 A g^{-1} are at least two times higher than those of polyaniline and its composites [35,36]. It is interesting to note that POT electrode can deliver notably high specific power of 3300 W kg^{-1} in the forced current regime of 13 A g^{-1}. The estimated values of the specific energy and power suggested that POT electrode could be considered as the battery type electrode at low currents. On the other hand, POT electrode can deliver significant power, exceeding 3 kW kg^{-1} at higher currents, similar to values characteristic for supercapacitor electrodes. The fast delivery of energy, i.e. power of POT, comparing to polyaniline, is probably a consequence of the faster dedoping reaction due to the presence of activating ortho positioned methyl group in the polymer structure.

As stated before, polyaniline suffers from low cycling stability demonstrated in loss of the charge capacity over cycling [6]. In order to examine cyclic stability of POT electrode, 2000 cycles of charge/discharge to discharge potential of 0.5 V and 0.4 V, at a specific current of 13.1 A g^{-1}, are performed and results are shown in Fig. 9.

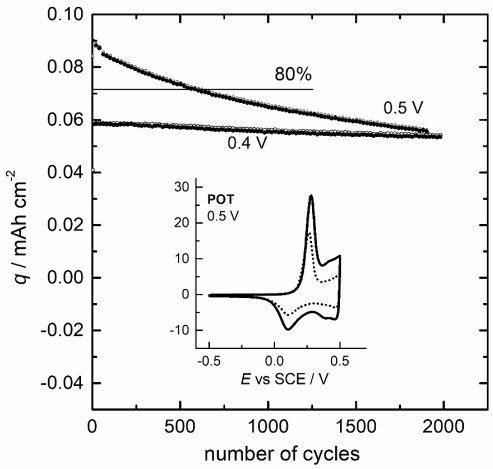

Fig. 9. The capacity of POT electrode over 2000 charge/discharge cycles at 13.1 A g^{-1}, to charge potential limits indicated on the figure, and discharge to –0.35 V. Insert: Cyclic

voltammogram of POT electrode, before (full line) and after (dash line) 2000 charge/discharge cycles to charge potential limit of 0.5 V.

As seen in Fig. 9 after about 600 charge/discharge cycles to the potential of 0.5 V, POT electrode retained 80 % of initial capacity and after completed 2000 cycles, the capacity loss is 40 % of the initial value. By the shape of cyclic voltammograms of POT electrode taken before and after charge/discharge to 0.5 V, it can be concluded that there are no changes in the nature of the charge/discharge process although the peak current characteristic to emeraldine like state decreased, suggesting possible loss of the active mass provoked by degradation of POT. On the other hand, by limiting the discharge potential to 0.4 V, capacity retention is over 90 % after 2000 cycles, which suggested good base for practical application.

4. Conclusions

Electrochemical formation of POT on graphite electrode is successively performed by galvanostatic polymerisation from an aqueous electrolyte containing 0.25 mol dm^{-3} of *o*-toluidine and 1.0 mol dm^{-3} H_2SO_4. Both cyclic voltammetry and Mott Schottky experiments revealed similar redox behavior to polyaniline with the transition from leucoemeraldine to emeraldine like state followed by an insulator to conductor transition induced by the increase of the potential. Specific energy between 17.5 Wh kg^{-1} and 12 Wh kg^{-1} and specific power between 300 W kg^{-1} to 3300 W kg^{-1} are both determined by integration of the charge/discharge curves, indicating excellent energy storage properties of POT electrode. By proper choice of the discharge potential limit, POT electrode retains over 90% of the initial capacity during 2000 charge/discharge cycles.

Acknowledgements

The research was supported by the Ministry of Education, Science and Technological Development of the Republic of Serbia, under the research project "Electrochemical synthesis and characterization of nanostructured functional materials for applications in new technologies" No. ON172046.

References

[1] L. Yu, G.Z. Chen, Redox electrode materials for supercapatteries, J. Power Sources. 326 (2016) 604–612. doi:10.1016/j.jpowsour.2016.04.095.

[2] T. Brousse, B. Daniel, To Be or Not To Be Pseudocapacitive ?, 162 (2015) 5185–5189. doi:10.1149/2.0201505jes.

[3] Y. Wang, J. Guo, T. Wang, J. Shao, D. Wang, Y.-W. Yang, Mesoporous Transition Metal Oxides for Supercapacitors, Nanomaterials. 5 (2015) 1667–1689. doi:10.3390/nano5041667.

[4] A.K. Shukla, A. Banerjee, M.K. Ravikumar, A. Jalajakshi, Electrochemical capacitors: Technical challenges and prognosis for future markets, Electrochim. Acta. 84 (2012) 165–173. doi:10.1016/j.electacta.2012.03.059.

[5] A.M. Bryan, L.M. Santino, Y. Lu, S. Acharya, J.M. D'Arcy, Conducting Polymers for Pseudocapacitive Energy Storage, Chem. Mater. 28 (2016) 5989–5998. doi:10.1021/acs.chemmater.6b01762.

[6] T. Liu, L. Finn, M. Yu, H. Wang, T. Zhai, X. Lu, Y. Tong, Y. Li, Polyaniline and polypyrrole pseudocapacitor electrodes with excellent cycling stability, Nano Lett. 14 (2014) 2522–2527. doi:10.1021/nl500255v.

[7] A. Eftekhari, L. Li, Y. Yang, Polyaniline supercapacitors, J. Power Sources. 347 (2017) 86–107. doi:10.1016/j.jpowsour.2017.02.054.

[8] A.A. Alguail, A.H. Al-Eggiely, B.N. Grgur, Polyaniline–lead sulfate based cell with supercapattery behavior, J. Saudi Chem. Soc. 21 (2017) 575–582. doi:10.1016/j.jscs.2017.01.002.

[9] A.A. Alguail, A.H. Al-Eggiely, M.M. Gvozdenović, B.Z. Jugović, B.N. Grgur, Battery type hybrid supercapacitor based on polypyrrole and lead-lead sulfate, J. Power Sources. 313 (2016). doi:10.1016/j.jpowsour.2016.02.081.

[10] L. Arsov, W. Plieth, G. Koßmehl, Electrochemical and Raman spectroscopic study of polyaniline; influence of the potential on the degradation of polyaniline, J. Solid State Electrochem. 2 (1998) 355–361.

[11] E. Mitchell, J. Candler, F. De Souza, R.K. Gupta, B.K. Gupta, L.F. Dong, High performance supercapacitor based on multilayer of polyaniline and graphene oxide, Synth. Met. 199 (2015) 214–218. doi:10.1016/j.synthmet.2014.11.028.

[12] K. Li, D. Guo, J. Chen, Y. Kong, H. Xue, Oil-water interfacial synthesis of graphene-polyaniline-MnO<inf>2</inf> hybrids using binary oxidant for high performance supercapacitor, Synth. Met. 209 (2015) 555–560. doi:10.1016/j.synthmet.2015.09.017.

[13] W. Tang, L. Peng, C. Yuan, J. Wang, S. Mo, C. Zhao, Y. Yu, Y. Min, A.J. Epstein, Facile synthesis of 3D reduced graphene oxide and its polyaniline composite for super capacitor application, Synth. Met. 202 (2015) 140–146. doi:10.1016/j.synthmet.2015.01.031.

[14] A. Vega-Rios, F.Y. Rentería-Baltiérrez, C.A. Hernández-Escobar, E.A. Zaragoza-Contreras, A new route toward graphene nanosheet/polyaniline composites using a reactive surfactant as polyaniline precursor, Synth. Met. 184 (2013) 52–60. doi:10.1016/j.synthmet.2013.09.014.

[15] J. Pinit, N. Paradee, A. Sirivat, Electrochromic characteristics of poly(o-toluidine) coated onto flexible indium tin oxide: Effect of H2SO4and 1-butyl-3-

methylimidazolium chloride electrolytes, Thin Solid Films. 616 (2016) 381–387. doi:10.1016/j.tsf.2016.08.057.

[16] J. Ju, X. Bo, H. Wang, Y. Zhang, C. Luhana, L. Guo, Poly-o-toluidine cobalt supported on ordered mesoporous carbon as an efficient electrocatalyst for oxygen reduction, Electrochem. Commun. 25 (2012) 35–38. doi:10.1016/j.elecom.2012.09.023.

[17] A. Elmansouri, A. Outzourhit, A. Lachkar, N. Hadik, A. Abouelaoualim, M.E. Achour, A. Oueriagli, E.L. Ameziane, Influence of the counter ion on the properties of poly(o-toluidine) thin films and their Schottky diodes, Synth. Met. 159 (2009) 292–297. doi:10.1016/j.synthmet.2008.10.001.

[18] D. Manoharan, J. Chandrasekaran, S. Maruthamuthu, P. Jayamurugan, Poly(aniline-co-o-toluidine): Poly(styrene sulfonic acid) nanocolloidal self assembled multilayer thin films as a hole transport layer in organic solar cells, Mater. Sci. Semicond. Process. 34 (2015) 382–389. doi:10.1016/j.mssp.2015.02.079.

[19] P. Ghosh, A. Chakrabarti, S.B. Kar, R. Chowdhury, Conducting blends of poly(o-toluidine) and poly(ester)urathane, Synth. Met. 144 (2004) 241–247. doi:10.1016/j.synthmet.2004.03.007.

[20] S. Bilal, S. Farooq, A.U.H.A. Shah, R. Holze, Improved solubility, conductivity, thermal stability and corrosion protection properties of poly(o-toluidine) synthesized via chemical polymerization, Synth. Met. 197 (2014) 144–153. doi:10.1016/j.synthmet.2014.09.003.

[21] P. Sambyal, G. Ruhi, H. Bhandari, S.K. Dhawan, Advanced anti corrosive properties of poly(aniline-co-o-toluidine)/flyash composite coatings, Surf. Coatings Technol. 272 (2015) 129–140. doi:10.1016/j.surfcoat.2015.04.013.

[22] S. Bilal, A. u H.A. Shah, R. Holze, A correlation of electrochemical and

spectroelectrochemical properties of poly(o-toluidine), Electrochim. Acta. 54 (2009) 4851–4856. doi:10.1016/j.electacta.2009.03.072.

[23] H. Gul, A.A. Shah, S. Bilal, Electrochemical behavior of POT in different electrolytes, 5 (2016) 187–192.

[24] B. Jugović, M. Gvozdenović, J. Stevanović, T. Trišović, B. Grgur, Characterization of electrochemically synthesized PANI on graphite electrode for potential use in electrochemical power sources, Mater. Chem. Phys. 114 (2009) 939–942. doi:10.1016/j.matchemphys.2008.10.069.

[25] G. Zotti, S. Cattarin, N. Comisso, Electrodeposition of polythiophene, polypyrrole and polyaniline by the cyclic potential sweep method, J. Electroanal. Chem. Interfacial Electrochem. 235 (1987) 259–273.

[26] J.E. De Albuquerque, L.H.C. Mattoso, R.M. Faria, J.G. Masters, A.G. MacDiarmid, Study of the interconversion of polyaniline oxidation states by optical absorption spectroscopy, Synth. Met. 146 (2004) 1–10. doi:10.1016/j.synthmet.2004.05.019.

[27] D. Yang, W. Lu, R. Goering, B.R. Mattes, Investigation of polyaniline processibility using GPC/UV–vis analysis, Synth. Met. 159 (2009) 666–674. doi:10.1016/j.synthmet.2008.12.013.

[28] B.M. Jokić, E.S. Džunuzović, B.N. Grgur, B.Z. Jugović, T.L. Trišovic, J.S. Stevanović, M.M. Gvozdenović, The influence of m-aminobenzoic acid on electrochemical synthesis and behavior of poly(aniline-co-(m-aminobenzoic acid), J. Polym. Res. 24 (2017). doi:10.1007/s10965-017-1313-5.

[29] B.S. Choi, S. Park, Electrochemical Growth of Nanosized Conducting Polymer Wires on Gold Using Molecular Templates **, Adv. Mater. (2010) 1547–1549.

[30] S. Choi, S. Park, Electrochemistry of Conductive Polymers XXVI . Effects of Electrolytes and Growth Methods on Polyaniline Morphology, (2002) 26–34.

doi:10.1149/1.1432675.

[31] L.H.. Mattoso, S.. Manohar, A.. MacDiarmid, A.. Epstein, Studies on the chemical syntheses and on the characteristics of polyaniline derivativesNo Title, J. Polym. Sci. Part A Polym. Chem. Banner. 33 (1995) 1227–1234.

[32] D. Li, R.B. Kaner, How nucleation affects the aggregation of nanoparticles, J. Mater. Chem. 17 (2007) 2279–2282. doi:10.1039/b700699c.

[33] Z. Wang, K.J. Aoki, J. Chen, X. Zeng, Frequency Dispersion of Double Layer Capacitance of Polyaniline-Coated Electrodes Under the Conducting State, Int. J. Chem. 10 (2018) 25–35. doi:10.5539/ijc.v10n2p25.

[34] A.Q. Contractor, V.A. Juvekar, Estimation of Equilibrium Capacitance of Polyaniline Films Using Step Voltammetry, 162 (2015) 1175–1181. doi:10.1149/2.0151507jes.

[35] Y. Yuan, W. Zhu, G. Du, D. Wang, J. Zhu, X. Zhu, G. Pezzotti, Electrochimica Acta Two-step method for synthesizing polyaniline with bimodal nanostructures for high performance supercapacitors, Electrochim. Acta. 282 (2018) 286–294. doi:10.1016/j.electacta.2018.06.006.

[36] K. Li, J. Liu, Y. Huang, F. Bu, Y. Xu, Integration of ultrathin graphene/polyaniline composite nanosheets with a robust 3D graphene framework for highly flexible all-solid-state supercapacitors with superior energy density and exceptional cycling stability, J. Mater. Chem. A. 5 (2017) 5466–5474. doi:10.1039/C6TA11224B.

Figure captions:

Fig. 1. Galvanostatic (1.5 mA cm^{-2}) electrochemical polymerization of *o*-toluidine in 0.25 mol dm^{-3} *o*-toluidine and 1.0 mol dm^{-3} H_2SO_4. Inset: UV-vis absorption spectra of POT.

Fig. 2. Formation of OT cation radicals at the anode.

Fig. 3. SEM micrographs of electrochemically synthesized POT at different magnifications.

Fig. 4. Cyclic voltammogram and capacitance and impedance at 1 Hz of POT electrode in 1.0 mol dm^{-3} H_2SO_4 in the potential range between –0.5 and 0.5 V.

Fig. 5. Emeraldine salt like state of POT with shared sulphate anions.

Fig. 6. Charge/discharge curves of POT electrode in 1.0 mol dm^{-3} H_2SO_4 with different current densities as marked in figure, a) over time and b) over recalculated capacity.

Fig. 7. The dependences of charge, q_{ch}, and discharge, q_{dch}, capacities on specific current. Insert: The dependence of Coulombic efficiency on specific current.

Fig.8. Ragone plot of POT electrode.

Fig. 9. The capacity of POT electrode over 2000 charge/discharge cycles at 13.1 A g^{-1}, to charge potential limits indicated on the figure, and discharge to –0.35 V. Insert: Cyclic voltammogram of POT electrode, before (full line) and after (dash line) 2000 charge/discharge cycles to charge potential limit of 0.5 V.

Highlights

- Electrochemical formation of poly(*o*-toluidine) (POT) electrode is successively achieved by galvanostatic polymerisation of *o*-toluidine from aqueous electrolyte.
- According to our knowledge, charge/discharge behaviour of POT electrode is performed for the first time.
- High values of both specific energy and power, together with high value of the specific capacity, are obtained.
- POT electrode is capable of retaining over 90% of the initial capacity over 2000 charge/discharge cycles.

electrochemical
polymerization
0.25 mol dm^{-3} *o*-toluidine
1.0 mol dm^{-3} H_2SO_4
j = 1.5 mA cm^{-2}
Q_{poly}= 1mAh cm^{-2}

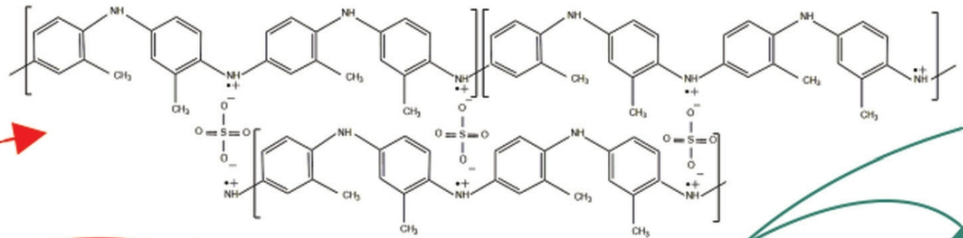

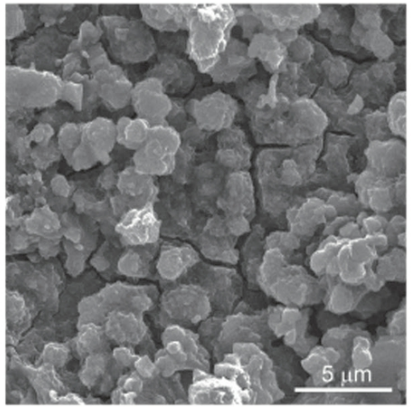

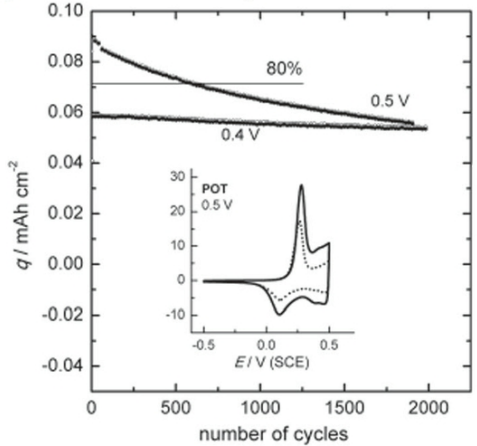

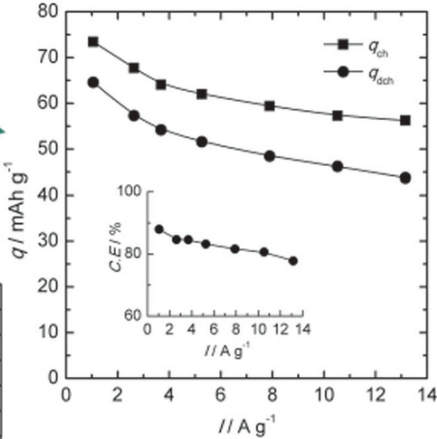

POT electrode
retain over 90%
of the initial capacity
during 2000
charge/discharge
cycle